POLYGONAL IMPACT CRATERS ON CHARON. C.B. Beddingfield[1,2], R. Beyer[1,2], R.J. Cartwright[1,2], K. Singer[3], S. Robbins[3], S.A. Stern[3], V. Bray[4], J.M. Moore[2], K. Ennico[2], C.B. Olkin[3], J.R. Spencer[3], H.A. Weaver[5], L.A. Young[3], A.Verbiscer[6], J. Parker[3], and the New Horizons Geology, Geophysics, and Imaging (GGI) Team; [1]SETI Institute, Mountain View, CA, [2]NASA Ames Research Center, Mountain View, CA (chloe.b.beddingfield@nasa.gov), [3]Southwest Research Institute, Boulder, CO, [4]University of Arizona, Tucson, AZ, [5]John Hopkins University Applied Physics Laboratory, Laurel, MD, [6]University of Virginia, Charlottesville, VA.

Introduction: Polygonal impact craters (PICs) reflect pre-existing extensional and strike-slip faults and fractures in the target material [e.g. 1-9]. PIC straight rim segments therefore can provide important information for deciphering the tectonic histories of planetary bodies [e.g. 8]. The only known PIC formation mechanism is the presence of pre-existing sub-vertical structures within the target material [e.g. 5, 7, 11-13].

In contrast, circular impact craters (CICs) are inferred to result from impact events in non-tectonized target material. CICs can also form in pre-fractured target material if the fractures are widely or closely spaced, if the fracture system is highly complex, or if the target material is covered by a thick layer of non-cohesive sediment that limits interactions between the impactor and the underlying bedrock/ice [e.g. 14]. Consequently, PICs and CICs are useful tools to distinguish between non-tectonized and tectonized terrains on the surfaces of both silicate- and ice-rich planetary bodies [e.g., 8-9].

The surface of Charon exhibits an abundance of impact craters [15, 16] overprinting Oz Terra in the North, as well as Vulcan Planitia in the south. Fractures and lineated textures are present in both regions, and have been attributed to extensional faulting and fracturing. Along with abundant examples of CICs, Charon appears to display many examples of PICs (Fig. 2a-d), but the plan-view geometries of these candidate PICs have not been quantified.

Data and Methods: In this project, we apply a technique to identify and analyze PICs on Charon, which we have used previously to identify PICs on icy bodies like Dione [8] and Miranda [9,10]. We are analyzing impact craters identified in New Horizons LORRI images. Image processing is being done using the USGS Integrated Software for Imagers and Spectrometers3 (ISIS3) [17]. Illumination geometry does not have a strong effect on the identification of PICs [18], and so we are able to use many of the available images.

All images are projected to the center of each crater to maximize the accuracy of geometry measurements. Craters overprinted by other craters or cut by faults are not analyzed. Additionally, we exclude craters chains/clusters and craters smaller than ~10 times the image resolution from our analysis.

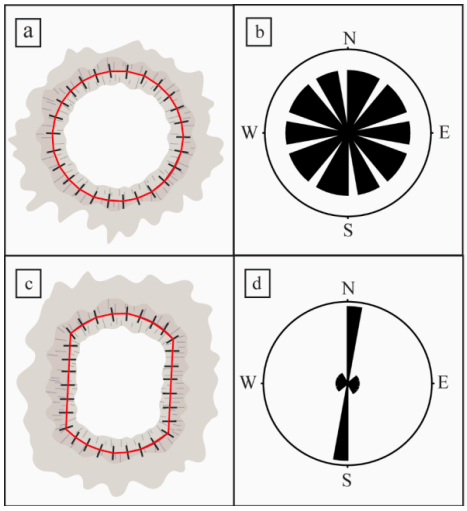

Fig. 1: *Plan view geometries of impact craters illustrating how rims are traced (red) and normalized to equal lengths (bounded by black tick marks), and the associated rose diagrams of their rim azimuth distributions. a) A circular impact crater (CIC). b) The CIC rose diagram, which shows a uniform crater rim azimuth distribution. c) A polygonal impact crater (PIC). d) The PIC rose diagram, which shows a non-uniform rim azimuth distribution, and a PIC azimuth of 0° to 10°.*

We manually trace the rims of all analyzed craters, normalizing each traced rim, and then break these traced rims into segments of equal length (Fig. 1). We then calculate the azimuth of each rim segment and generate rose diagrams for each crater's azimuth distribution.

To identify PICs, we are testing for non-uniform azimuth distributions for each crater, using the Pearson's Chi-squared test [19]. Our null hypothesis is that the azimuth distribution for each crater is uniform (i.e., consistent with CICs), and we set the associated p-value to 0.05. Craters that reject this null hypothesis are identified as PICs. Next, we determine whether identified PICs reflect one or multiple straight rim segments using a Dip test [e.g. 20]. We then identify the prominent unimodal (single straight rim segment) or bimodal orientations for each PICs (the Dip test cannot assess significance beyond two modes). Thus, each PIC could reflect one or two fracture sets with different azimuths.

Preliminary Results and Discussion: Our preliminary results indicate that PICs are present in, and proximal to, the fractured and rilled terrain in Vulcan Planitia,

just south of Serenity Chasma. These PICs exhibit straight segments that parallel the rills (Fig. 2b).

Because PICs form in the presence of pre-existing tectonic structures, the presence of Charon's PICs, and the orientations of their straight rim segments, supports the interpretation by [21-23] that the subtle rilles are tectonic features, likely extensional graben. In addition, these PICs indicate that the rilles predate the craters, suggesting that the formation of the rilles occurred shortly after the formation of Vulcan Planitia, but before many subsequent impact events took place.

PICs are also present further south, adjacent to Clark Montes (Fig. 2c). To the north of Clark Montes, PIC straight rim segments parallel prominent fractures oriented approximately E-W. In addition, some straight rim segments indicate that a subtle NE-SW fracture system is present in this region, both to the north and west of Clark Montes. The presence of this NE-SW fracture system is also indicated by PIC straight rim segment orientations to the east, near Kubrick Mons (Fig. 2d).

Future Work: We will apply our methodology to impact craters on Charon that meet our selection criteria described above. We will identify and analyze PICs, and further investigate the fracture systems that formed them, across Charon. This work will therefore provide valuable information about Charon's tectonic history.

Acknowledgments: We thank NASA for financial support of the New Horizons project.

References: [1] Fielder (1961) *Plan. & Space Sci., 8, 1-8.* [2] Kopal (1966) An Intro. to the Study of the Moon, *Astro. and Space Sci. Lib.* [3] Shoemaker (1962) Interp. of lunar craters, *Phys. and Astron. of the Moon, 283-359.* [4] Shoemaker (1963) *The Moon, Meteor., and Com., 301-336.* [5] Roddy (1978) *LPSC., 9. 3891-3930.* [6] Öhman et al. (2005) Impact Tectonics, *Springer, 131-160.* [7] Öhman et al. (2009) The struct. control of impact craters, *Ph.D. diss.* [8] Beddingfield et al., (2016) *Icarus, 274, 163-194.* [9] Cartwright and Beddingfield (2020) *LPSC, 51, 1120.* [10] Beddingfield and Cartwright (2020) *Icarus, in prep.* [11] Fielder (1965) Lunar Geology, *Lutt. Press.* [12] Eppler et al. (1983) *Geol. Soc. Amer. Bull., 2, 274-291.* [13] Aittola et al., (2010) *Icarus, 205(2), 356-363.* [14] Fulmer and Roberts (1963) *Icarus, 2, 452-465.* [15] Robbins et al. (2017) *Icarus, 287, 187-206.* [16] Singer et al. (2019) *Science, 363, 955-959.* [17] Anderson et al. (2004) *Lunar Planet. Sci.* 35, 2039. [18] Öhman et al. (2006) *Met. & Plan. Sci., 41, 1163-1173.* [19] Burt et al. (2009) Elem. Stat. for Geog. *Guilford Press.* [20] Hartigan and Hartigan (1985) *An. of Stat., 70-84.* [21] Moore et al. (2016) *Science 351, 1284-1293.* [22] Beyer et al. (2017) *Icarus, 287, 161-174.* [23] Beyer et al. (2019) *Icarus, 323, 16-32.*

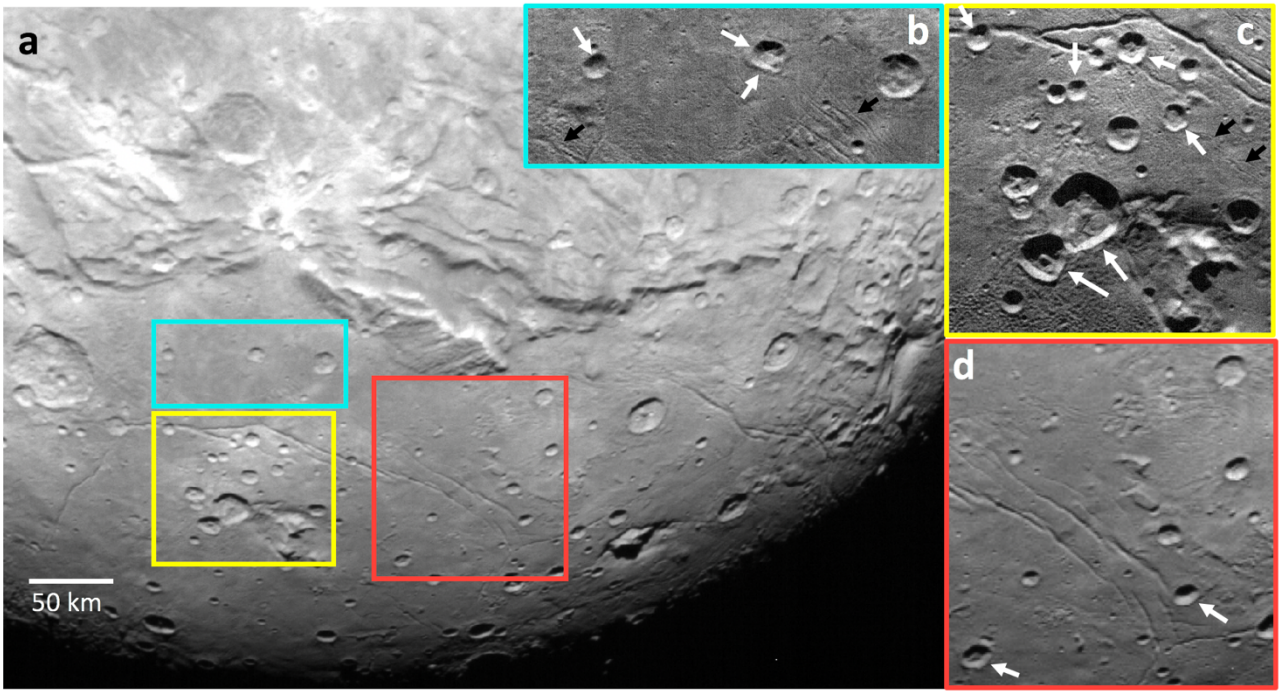

Fig. 2*: Locations of some PICs on Charon. Arrows show examples of nearby rilles (black) and PIC straight rim segments (white), which indicate pre-existing fracture orientations in the target material. Images are not projected in this figure. a) LORRI image lor_0299171413 showing locations of b, c, and d. b) A portion of lor_0299180418 that shows Clark Montes (bottom right) and the surrounding craters. The straight rim segments of PICs exhibit straight rim segments that parallel nearby rills (bottom). c) A portion of lor_0299175682 to the west of Kubrick Mons. d) A portion of lor_0299180421.*